Measuring Atmospheric CO_2 Enhancements from the 2017 British Columbia Wildfires using a Lidar

Jianping Mao*[1,2], James B. Abshire[1,2], S. Randy Kawa[2], Haris Riris[2], Xiaoli Sun[2], Niels Andela[3] and Paul T. Kolbeck[1]

1. University of Maryland at College Park; 2. NASA Goddard Space Flight Center; Greenbelt, MD 20771, USA; 3. Cardiff University, UK

Correspondence to: Jianping.Mao@nasa.gov

Abstract. During the summer 2017 ASCENDS/ABoVE airborne science campaign, the NASA Goddard CO_2 Sounder lidar overflew smoke plumes from wildfires in the British Columbia, Canada. In the flight path over Vancouver Island on 8 August 2017, the column XCO_2 retrievals from the lidar measurements at flight altitudes around 9 km showed an average enhancement of 4 ppm from the wildfires. A comparison of these enhancements with those from the Goddard Global Chemistry Transport model suggested that the modeled CO_2 emissions from wildfires were underestimated by more than a factor of 2. A spiral-down validation performed at Moses Lake airport, Washington showed a bias of 0.1 ppm relative to *in situ* measurements and a standard deviation of 1 ppm in lidar XCO_2 retrievals. The results show that future airborne campaigns and spaceborne missions with this type of lidar can improve estimates of CO_2 emissions from wildfires and estimates of carbon fluxes globally.

Plain Language Abstract. Wildfires are a major source of greenhouse gases. However, there are large uncertainties in the estimated CO_2 emissions from wildfires in global emissions inventories. The estimates of column-averaged CO_2 (XCO_2) from satellite measurements using passive remote sensing techniques are significantly degraded or screened out by the scattering from smoke in the scene. NASA Goddard Space Flight Center has developed an integrated-path, differential absorption lidar approach to measure XCO_2 from space. Measurements of time-resolved laser backscatter profiles from the atmosphere allow this technique to accurately estimate XCO_2 and range to terrain and water surfaces even in the presence of wildfire smoke. We demonstrate this capability over Vancouver Island through the dense smoke plumes from wildfires in the Canadian Rockies during the summer 2017 ASCENDS/ABoVE airborne science campaign. To our knowledge this is the first use of lidar to remotely sense CO_2 enhancements from large wildfires. Future airborne campaigns and spaceborne missions with this capability can improve estimates of CO_2 emissions from wildfires and help estimates of carbon fluxes globally.

Key Points:

- NASA Goddard CO_2 Sounder Lidar can accurately measure CO_2 enhancements from wildfires through dense smoke plumes
- This is the first use of lidar to remotely sense CO_2 enhancements from large wildfires

- These types of lidar measurements can be used to validate estimates of CO_2 emissions from wildfires and improve estimates of carbon fluxes

1. Introduction

Wildfires are a major source of greenhouse gases. Fires were responsible for as much as a fifth of the carbon released in 2019 from burning fossil fuels, down from about a quarter at the beginning of the century (Ciais et al., 2013; Tian et al., 2016; Le Quere et al., 2018). While this long-term decrease in fire emissions was driven by a decline in savanna and grassland fires (Andela et al., 2017), a recent increase in forest fires has resulted in concerns about the future role of fire in the global carbon cycle. Total carbon emissions from forest fires in 2019 were 26% higher than in 2018, to 7.8 billion metric tons, the highest since 2002, according to the Global Fire Emissions Database (GFED; van der Werf et al., 2017). The unprecedented bushfires in Australia in 2019 emitted a combined 306 million metric tons of carbon dioxide (CO_2) in the August-December 2019 period, which is more than half of Australia's total carbon footprint in the year. Brazilian Amazon fires emitted 392 million metric tons of CO_2 in 2019 which was equivalent to more than 80% of Brazil's 2018 greenhouse gas emissions (Lombrana et al., 2020).

During 2017 Canada had a record-breaking wildfire season in the province of British Columbia (BC). A total of 1.2 million hectares had burned by the end of the 2017 fire season, the largest ever in the province (Duran, 2017) and massive smoke plumes were lofted into the stratosphere in the mid-August (Torres et al., 2020).

Generally, there are large uncertainties in the estimated CO_2 emissions from wildfires with fire emissions inventories (Meyer et al., 2012; Andreae, 2019). Ground-based and airborne measurements of fire emissions are few and are difficult to obtain. Atmospheric column-averaged dry air mole fraction of CO_2 (XCO_2) retrievals using surface reflected sunlight, e.g., the Orbiting Carbon Observatory-2 (OCO-2; Crisp et al., 2004) and the Greenhouse gases Observation SATellite (GOSAT; Kuze et al., 2016) are significantly degraded by scattering effects of fire smoke in the scene (Mao and Kawa, 2004; Houweling et al., 2005; Aben et al., 2007; Butz et al., 2009; Uchino et al., 2012; Guerlet et al., 2013).

NASA Goddard Space Flight Center has developed an integrated-path, differential absorption (IPDA) lidar approach to measure global XCO_2 from space as a candidate for NASA's planned Active Sensing of CO_2 Emissions over Nights, Days, and Seasons (ASCENDS) mission (Kawa et al., 2018). This pulsed laser approach uses a step-locked laser source and a high-efficiency detector to measure atmospheric absorption at multiple wavelengths across the CO_2 line centered at 1572.335 nm. It has a high spectral resolution and sub-ppm sensitivity to changes in XCO_2 (Abshire et al., 2018). Measurements of time-resolved atmospheric backscatter profiles allow this technique to estimate XCO_2 and range to any significant reflective surfaces with precise knowledge of the photon path-length even in the presence of atmospheric scattering (Ramanathan et al., 2015; Mao et al., 2018).

During July and August 2017, NASA conducted a joint ASCENDS/ABoVE (Arctic Boreal Vulnerability Experiment) airborne science campaign using the NASA DC-8 aircraft based in Fairbanks, Alaska (Mao et al., 2019). The CO_2 Sounder lidar measured

XCO_2 from aircraft altitudes to ground, along with height-resolved backscatter profiles. Other instruments on the DC-8 aircraft included the NASA Langley Research Center ACES CO_2 lidar (Obland et al., 2018) along with a suite of *in situ* instruments including AVOCET for CO_2 (Halliday et al., 2019), Picarro for CO_2, CH_4, and H_2O, and an engineering test version of DLH for H_2O, CO, CH_4, and N_2O (Diskin et al., 2002). The DC-8 aircraft's housekeeping data provided temperature, pressure, geolocation, and positioning such as altitude and pitch/roll angles at flight altitude. Its radar altimeter also provides a reference for ground elevation under all conditions since the radar measurement penetrates clouds and smoke.

During the return flight from Alaska to California on August 8 the aircraft overflew dense smoke plumes from fires in the Canadian Rockieson the segment from Vancouver Island to central Washington State. Here we present the XCO_2 and backscatter measurements over this region along with the validation spiral maneuver at Moses Lake airport in central Washington, performed shortly after the region of XCO_2 enhancement. We then compare the measured XCO_2 enhancements with those from the Goddard Parameterized Chemistry Transport Model (PCTM) using GFED. This case study demonstrates the capability of the CO_2 Sounder lidar approach to measure enhanced XCO_2 through dense smoke plumes, which allows improving the estimates of CO_2 emissions from wildfires.

2. Lidar Measurements from 2017 ASCENDS/ABoVE Airborne Science Campaign

2.1 2017 ASCENDS/ABoVE Airborne Campaign to Alaska

The CO_2 Sounder lidar has flown on DC-8 five times since 2010 over a variety of sites in the US, along with other ASCENDS airborne lidar candidates and *in situ* CO_2 sensors (Abshire et al., 2013, 2016, and 2018). The ASCENDS/ABoVE airborne science campaign to Alaska was the first to extend these lidar measurement to the arctic region. The 2017 campaign also allowed determining the horizontal gradients in XCO_2 during the long transit flights between California and Alaska. In all, eight flights were conducted over the Central Valley of California, the Northwest Territory Canada, and south and central Alaska between July 20 and August 8, 2017. Forty-seven vertical spiral maneuvers were conducted over a variety of atmospheres and surface types like desert, vegetation, permafrost, and both the Pacific and Arctic Oceans. The XCO_2 retrievals from the lidar measurements were validated against those computed from *in situ* measurements of CO_2 vertical profiles made during the spiral maneuvers.

The final flight of the campaign was conducted on August 8, 2017, based out of Fairbanks, AK and transited south back to Palmdale, CA (Figure 1, top panel). The flight had six spiral-down maneuvers when over land including ones at Northway airport in Alaska, Whitehorse airport in Yukon, Canada, Moses Lake airport in Washington, Wildhorse airport in Oregon, Winnemucca airport in Nevada, and Edwards Air Force Base in California. The flight also conducted two in-line descent-ascent maneuvers above the Pacific Ocean just off the southern tip of Alaska before flying to Vancouver Island. Other than the spirals, almost all the flight was at 8-9 km altitude, except for the final segment between Reno NV and Edwards CA, which was flown at 12 km to allow sampling upper tropospheric air.

The bottom panel of Figure 1 shows *in situ* CO_2 concentrations at aircraft altitudes measured by AVOCET for the flight. AVOCET has a stated precision of ±0.1 ppm (1-sigma) and accuracy of ±0.25 ppm (Halliday et al., 2019). It shows significant horizontal and vertical gradients of CO_2 at the aircraft altitude, which is a typical seasonal pattern in the area. The CO_2 concentrations were higher near the surface at Fairbanks, Northway, and Whitehorse airports during the morning time of the flight due to the overnight accumulation of respiration and local emissions. Meanwhile, the higher CO_2 over Winnemucca, NV and Edwards Air Force Base, CA were presumably due to regional emissions, as there is little surface uptake over the deserts. The *in situ* measurements show high CO_2 in the free troposphere during the flight segment over Pacific Ocean and lower CO_2 in the following segment onto land before the spiral at Moses Lake, WA. It was notable that no outstanding CO_2 enhancements were seen at the aircraft altitude between the spirals at Pacific 2 and Moses Lake compared to CO_2 values at the same flight altitude before and after the segment.

2.2 XCO_2 Measurements from the CO_2 Sounder Lidar

The airborne CO_2 Sounder lidar uses a tunable laser to measure absorption across the vibration–rotational line of CO_2 centered at 1572.335 nm (Abshire et al., 2018). The lidar transmits 1-µs wide laser pulses at a rate of 10 kHz and the laser is stepped in 30 wavelengths across the CO_2 line at a rate of 300 Hz. The wavelength separation of each laser pulse was 250 MHz near line center and increased to 2 GHz at line wings to allow for more online samples. The laser line width is narrower than 30 MHz. The spectral resolution of the laser is over two hundred times higher than that of GOSAT, over three hundred times higher than that of OCO-2, and over twenty times higher than that of the ground-based Fourier Transform Spectrometers for the Total Carbon Column Observing Network (Wunch et al., 2011). The high spectral resolution allows sampling the fully-resolved CO_2 line shape, including line width and line center position (Ramanathan et al., 2013), resulting in high sensitivity to CO_2 changes in the atmospheric column (Mao and Kawa, 2004).

The lidar retrieval algorithm uses a least-squares fit between the 30 wavelengths of the lidar measurements and the calculated CO_2 absorption line shape to retrieve XCO_2 (Ramanathan et al., 2018; Sun et al., 2021). The approach allows use of a standard linear least squares method to simultaneously solve for Doppler frequency shift, surface reflectance at off-line wavelengths, and a linear non-uniformity (slope) in the receiver spectral response as well.

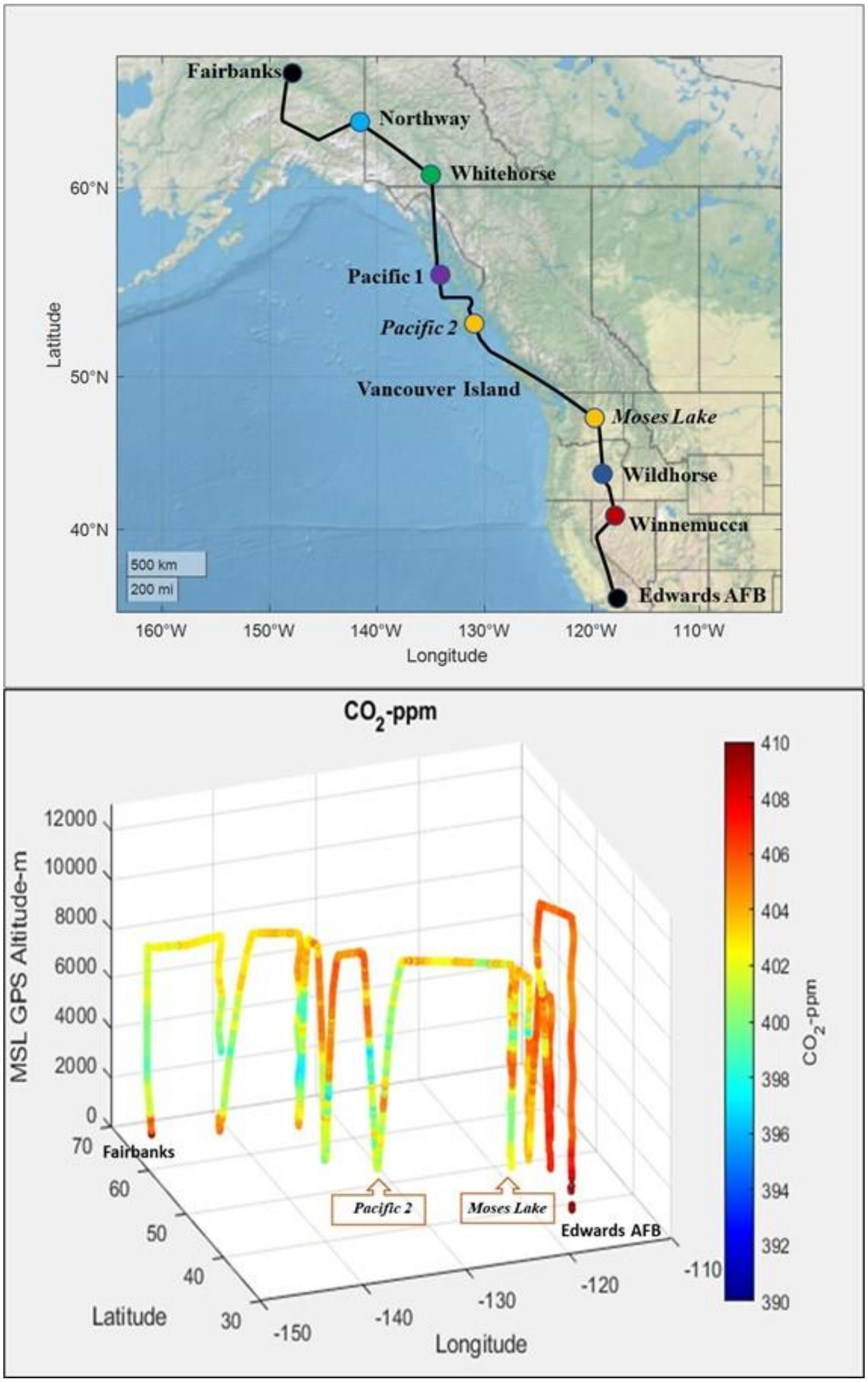

Figure 1. *Top*: map of the ground track for the return flight from Fairbanks, AK to Palmdale, CA on August 8, 2017. Fairbanks and the locations of eight spiral down flight segments are marked in circles, including two in-line descent-ascent maneuvers over Pacific Ocean labeled as Pacific 1 & Pacific 2. *Bottom*: 3-D (latitude, longitude, and flight altitude) sideview of *in situ* CO_2 mixing ratio measurements from onboard AVOCET for this flight. The data were sampled at 1-s intervals.

In the retrieval forward calculations, the spectroscopy database HITRAN 2008 (Rothman et al., 2009) and the Line-By-Line Radiative Transfer Model (Clough et al., 1992; Clough and Iacono, 1995) V12.1 were used to calculate CO_2 optical depth and create look-up tables (LUTs) for a prior with a vertically uniform CO_2 concentration of 400 ppm. We then used these LUTs to retrieve the best-fit XCO_2 by comparing the lidar sampled line shapes with the calculated absorption line shapes and then scaling the prior without any inversion constraints. The retrievals used the atmosphere state (pressure, temperature, and water vapor profiles) from the near real time forward processing data of the Goddard Earth Observing System Model, Version 5 (GEOS-5; Rienecker et al., 2011). Data on the full model grid (0.25° latitude×0.3125° longitude×72 vertical layers, every 3h) were interpolated to flight ground track position and time for the atmospheric CO_2 and H_2O absorption calculations.

3. Data Analysis Results

3.1 CO_2 Enhancements from BC Wildfires

Figure 2(a) shows the cloud-free XCO_2 retrievals from the lidar for the entire flight on August 8, 2017. Significant XCO_2 enhancements were clearly seen in the segment over Vancouver Island and across the Strait of Juan de Fuca into Washington State. Such CO_2 enhancements were not evident in the *in situ* measurements at flight altitudes (Fig. 1). Compared to single-point *in situ* measurements, this shows a benefit of the lidar's XCO_2 measurements to capture CO_2 variations in the full atmospheric column below the aircraft.

The smoke plumes from wildfires in the Canadian Rockies were clearly seen from DC-8 aircraft over Vancouver Island and the fire and thermal anomalies map from Aqua/MODIS on the same day (Figure 2(b) and (c)). The smoke plumes were transported by wind from the Canadian Rockies into eastern Washington State and further down into Montana. Meanwhile, some smoke plumes and a large amount of CO_2 emissions from the fires were also transported to Vancouver Island.

Figure 3 shows the time series of the cloud-free XCO_2 retrievals together with the attenuated backscatter profiles for the flight segment from Pacific Ocean to Washington State. Dense smoke layers were seen in the lidar backscatter profiles near Vancouver Island and peaked at the top of the boundary layer near 2 km. The lidar range was used to distinguish ground returns from cloud returns after comparison to onboard radar altimetry. The XCO_2 retrievals over Vancouver Island and western Washington State have a median value of 406.5 ppm. The XCO_2 computed from the *in situ* vertical profiles of CO_2 mixing ratio during the spiral maneuvers at Pacific 2 and Moses Lake were 401.9 and 402.6 ppm, respectively. Therefore, the averaged XCO_2 enhancement within the segment from Vancouver Island to western Washington State was estimated to be 4 ppm. The XCO_2 enhancement segment spanned about 30 minutes, which at DC-8 aircraft speed of 200 m/s, corresponds to a ground-track length of 360 km.

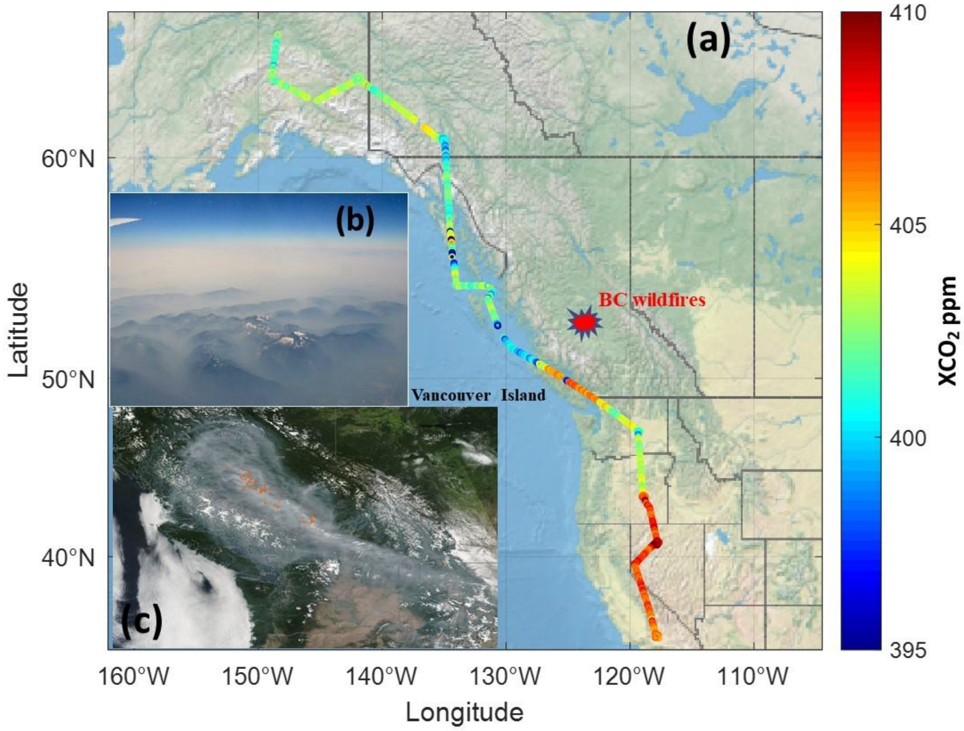

Figure 2. (a) the cloud-free XCO_2 retrievals from the CO_2 Sounder lidar for the flight on August 8, 2017. Significant XCO_2 enhancements were seen in the flight segment crossing Vancouver Island. The British Columbia wildfires are marked to the north of these enhancements. (b) image of the smoke plumes from the wildfires in Canadian Rockies as seen from DC-8 over Vancouver Island (Photo by Graham Allan). (c) true color image from Aqua/MODIS showing the smoke and fires on the same day.

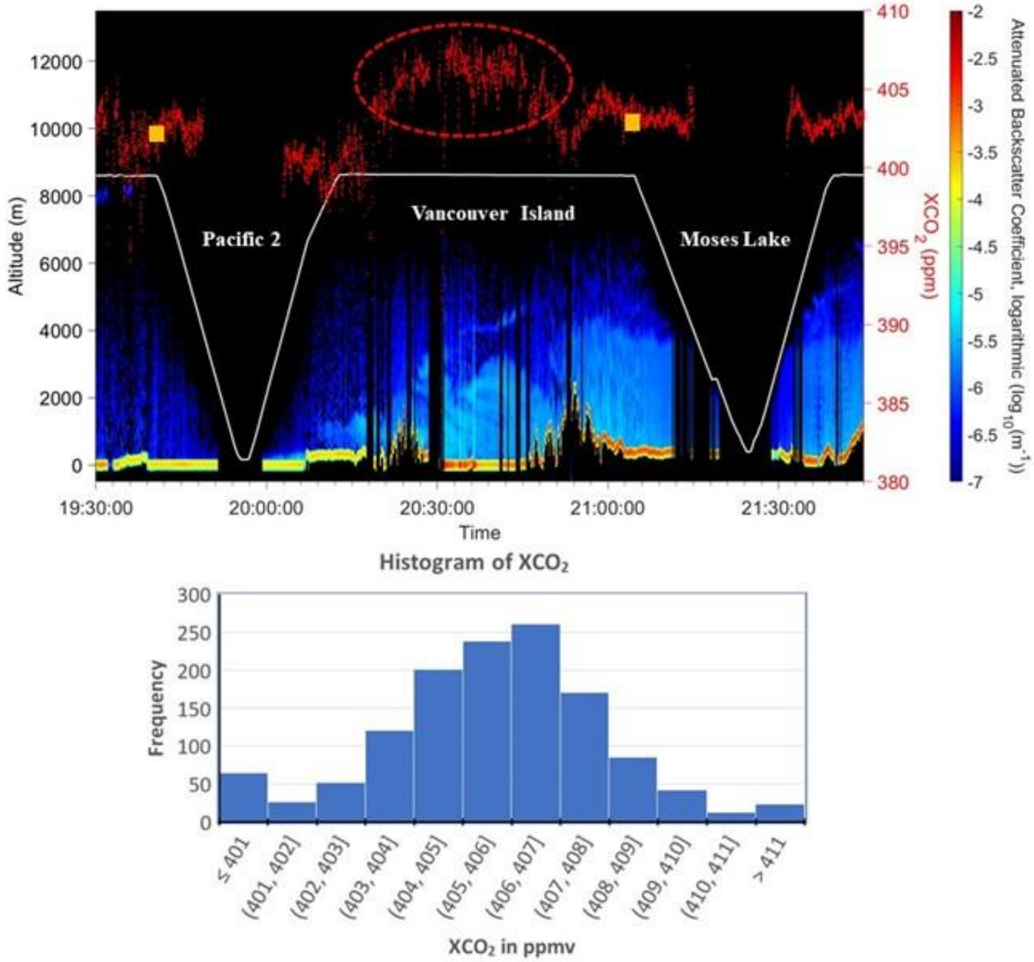

Figure 3. *Top*: the time series of cloud-free XCO_2 retrievals from the 1-s averaged lidar data (right axis) and the range-corrected attenuated backscatter profiles sampled at a vertical resolution of 15-m. Ground returns are strong and colored in yellow and red, and the returns from aerosols are light blue. The red dots are the 1-s XCO_2 retrievals smoothed with 9-point running mean. Aircraft GPS flight altitudes are marked in a white line. For reference, orange squares are the *in situ* XCO_2 from AVOCET during the 2nd in-line descent-ascent maneuver over Pacific Ocean and the spiral down maneuver at Moses Lake airport, Washington. The XCO_2 enhancements near Vancouver Island are circled. *Bottom*: a histogram of the 1-s averaged XCO_2 retrievals in the enhancement segment.

3.2 Validation of the Lidar XCO_2 Measurements

A vertical spiral-down maneuver was conducted shortly after the CO_2 enhancement segment shown in Fig. 3 from a flight altitude of 9 km to ground over Moses Lake in central Washington State. This allowed a comparison between the XCO_2 retrievals from the lidar and those constructed from the *in situ* vertical profile of CO_2. During the spiral hazy conditions were seen below 4.5 km in the lidar backscatter profiles (Fig. 3). The

AVOCET analyzer sampled every 1-s and the lidar XCO_2 retrievals were also based on 1-s averaged laser signals returned from ground. For the best estimation of the atmosphere state during the spiral maneuver, these retrievals used vertical profiles simultaneously measured by onboard DC-8 *in situ* instruments at an interval of 1-s. The *in situ* XCO_2 was computed from the *in situ* vertical profile integrated using the lidar's retrieval averaging kernel as vertical weighting. Both lidar and *in situ* XCO_2 were then averaged in each 1-km atmosphere layer for comparison. Figure 4 shows an average difference of less than 0.1 ppm for flight altitudes above 5-km and an average standard deviation of approximately 1 ppm. Validation results from other profiles throughout the campaign were within +/- 0.5 ppm (1-sigma) of the *in situ* data. Therefore, the 4 ppm XCO_2 enhancement from the Canadian wildfires was highly significant in relative to the lidar measurement uncertainty.

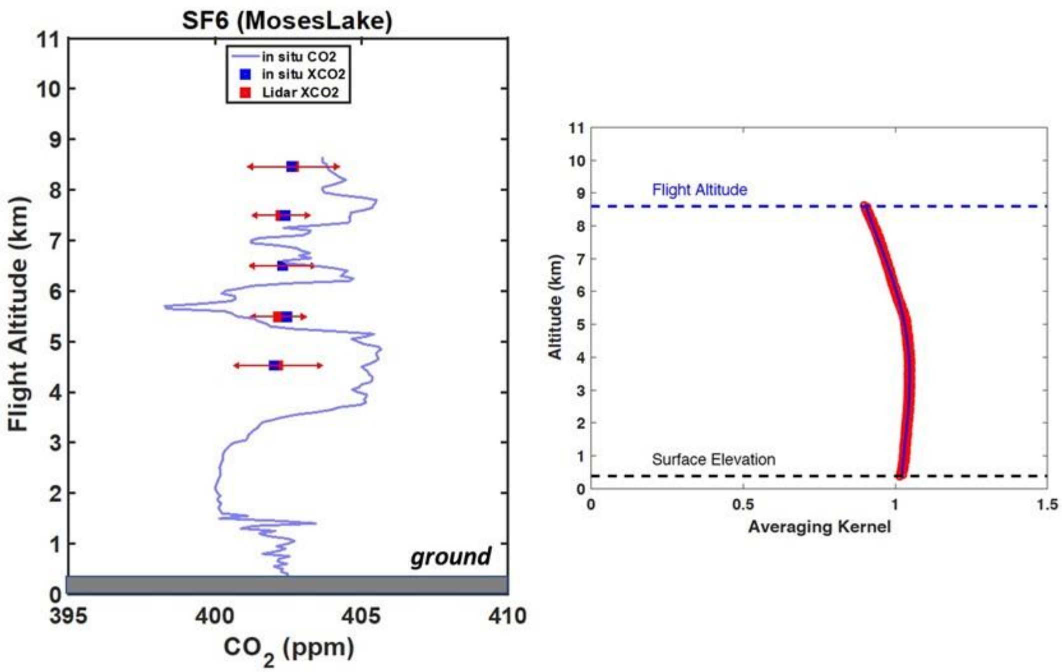

Figure 4. Comparison of cloud-free lidar XCO_2 retrievals with those from *in situ* measurements as a function of flight altitude during the spiral maneuver at Moses Lake, WA on August 8, 2017. The *in situ* XCO_2 values are marked in blue squares and the lidar's XCO_2 retrieval values are marked in red squares. The red error bars are ±1 standard deviation of the lidar's XCO_2 retrievals. The XCO2 vertical averaging kernel for this profile segment is shown at right.

3.3. Improving Estimates of CO_2 Emissions from Wildfires

Figure 5 shows the integrated XCO_2 below 320 mb (~ 9 km) from CO_2 simulations by the Goddard PCTM (Kawa et al., 2004 and 2010) on the same day. Note that averaging kernels were not applied to the model XCO_2 for estimating relative changes due to fire emissions. The PCTM CO_2 simulation is driven by meteorological data from the Modern-

Era Retrospective analysis for Research and Applications (Bosilovich, 2013), which is a NASA reanalysis using GEOS-5. The vertical mixing in PCTM is parameterized for both turbulent diffusion in the boundary layer and convection. PCTM is run at 0.625° longitude×0.5° latitude with 56 hybrid vertical levels and outputs hourly. PCTM uses GFED4s (including small fires) for the CO_2 emissions from wildfires. GFED includes an ecosystem model that uses satellite observations of burned area and ecosystem productivity to estimate fuel loads and combustion (van der Werf et al., 2017).

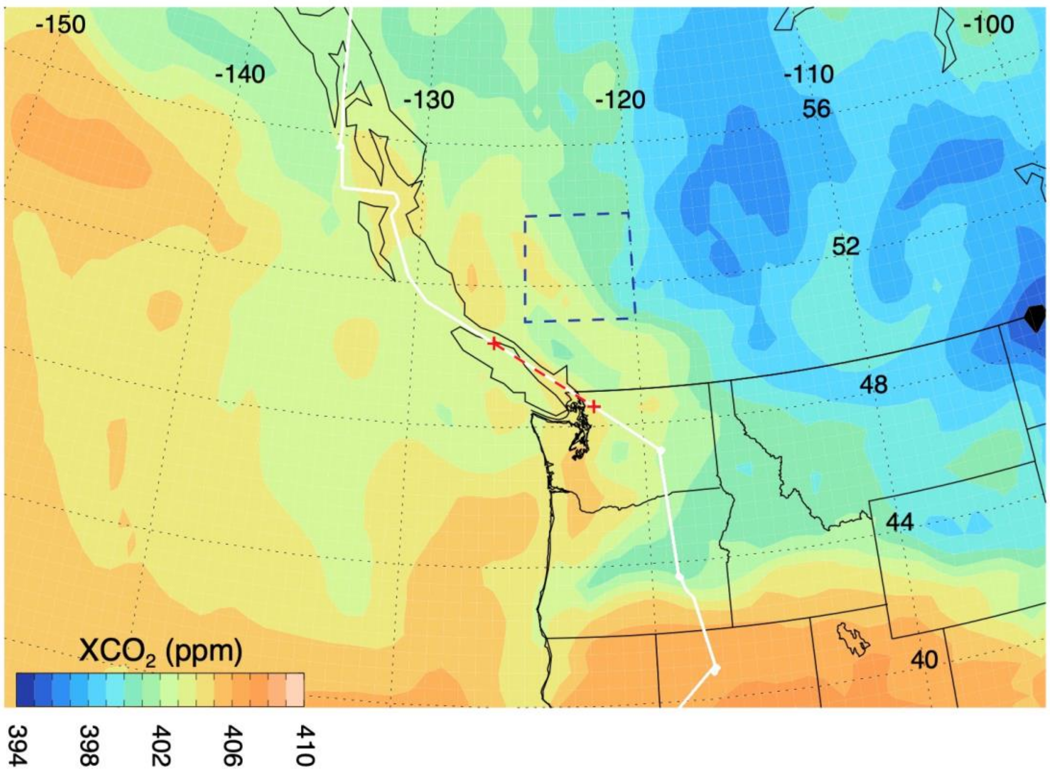

Figure 5. Map of XCO_2 (ppm) from ground to 320 mb simulated by Goddard PCTM at 21 GMT on August 8, 2017. White line is the ground track of the airborne campaign flight and the two red pluses and red dashed line mark the flight segment where the XCO_2 enhancements were seen in the lidar retrievals. The box delineated by the dashed blue line indicates the area over which the BC fire emissions were calculated.

The modeled XCO_2 at 21 GMT shows enhancements up to ~2 ppm over the Canadian Rockies in response to a total release of 837 Gg C day^{-1} from the BC fires within the area (51-54°N, 120-125°W) on August 8 estimated by GFED. The modeled XCO_2 enhancements near Vancouver Island (estimated from the local maximum on the contour map near the flight track in Figure 5 as well as from the model-interpolated XCO_2 along the track similar to Figure 3) were about 1 ppm. Compared to 4 ppm averaged enhancement of lidar XCO_2 for the equivalent atmospheric columns, the modeled enhancements were low. The underestimate of XCO_2 in the model could be due in part to model diffusion and transport shortcomings. Given, however, the spatial scale of the observed XCO_2 perturbation (~360 km) and multi-day duration of the fires, along with past performance of PCTM using analyzed winds to simulate CO_2 gradients in frontal systems and other relatively fine-scale features (Parazoo et al., 2008) as well as the parent GEOS-5 model use for aerosol plume simulations, we expect that the XCO_2 perturbation would be close to that observed if the emissions were correct. The daily CO_2 release estimate from another dataset of fire emissions, the Quick Fire Emissions Dataset (QFED; Darmenov and Silva, 2015), in the same area on the same day was 1122 Gg C day^{-1}. The QFED estimate was 34% higher than that from GFED but proportionally still underestimated at least by a factor of 2. QFED is based on the detection of fire radiative power calibrated against observations of aerosol optical depth. Our findings in this case study highlight the potential of airborne and spaceborne lidar XCO_2 measurements for evaluating atmospheric models and global emissions inventories.

4. Conclusion and Discussion

Analysis of lidar measurements from the summer 2017 ASCENDS/ABoVE airborne science campaign show the capability to measure XCO_2 enhancements through dense smoke plumes from wildfires in British Columbia, Canada. On the overpass of Vancouver Island on August 8, the retrievals from the lidar measurements showed an average 4 ppm enhancement in XCO_2 beneath the aircraft. A spiral maneuver made after the smoke plume showed the XCO_2 measurements had small bias and high precision, and a high spatial resolution (~ 200-m). The modeled enhancements from the Goddard PCTM which uses the GFED fire emission database were about 1 ppm near Vancouver Island. The result suggests that the CO_2 emissions from GFED for the BC wildfires were underestimated by a factor of 2 or more for that day.

The results show that future airborne campaigns and spaceborne missions with this capability should improve modeling of CO_2 emissions from wildfires. This will benefit atmospheric transport process studies, carbon data assimilation, and global and regional carbon flux estimates. Along with the expected increase in the net contribution of forest fires to global carbon emissions, improved capabilities to constrain wildfire emissions is greatly needed.

5. Acknowledgements: This work was supported by the NASA ASCENDS pre-formulation activity, the ABoVE project, and the Airborne Science Program. We gratefully acknowledge the work of the DC-8 team at NASA Armstrong Flight Center for helping plan and conduct the flight campaign. We also thank Joshua P. DiGangi, Glenn Diskin and Yonghoon Choi from NASA Langley Research Center for providing the *in situ* CO_2 and H_2O data. All the data used in this work can be downloaded at the LaRC airborne science data site, https://www-air.larc.nasa.gov/cgi-bin/ArcView/ascends.2017. This paper is dedicated to our friend and colleague Dr. Graham R. Allen who had a key role in the 2017 ASCENDS/ABoVE airborne campaign but who passed away in May 2020. Dr. Allen's work was essential in the development of the Goddard CO_2 Sounder lidar, airborne campaigns, and data analysis over the past decade and he is missed. We thank two anonymous reviewers whose edits and comments/suggestions helped improve and clarify this manuscript.

6. References

Aben, I., O. Hasekamp, and Hartmann, W.: Uncertainties in the space-based measurements Of CO_2 columns due to scattering in the Earth's atmosphere, J. Quant. Spectrosc. Radiat. Transfer, 104, 450-459, 2007.

Abshire, J.B., Riris, H., Allan, G.R., Weaver, C.J., Mao, J., Sun, X., Hasselbrack, W.E., Kawa, S.R., Biraud, S.: Pulsed airborne lidar measurements of atmospheric CO_2 column absorption. Tellus, 62, 770–783, 2010.

Abshire, J. B., Riris, H., Weaver, C. W., Mao, J., Allan, G. R., Hasselbrack, W. E., Weaver, C. J., Browell, E. W.: Airborne measurements of CO_2 column absorption and range using a pulsed direct-detection integrated path differential absorption lidar, Appl. Opt. 52, 4446-4461, 2013.

Abshire, J. B., Ramanathan, A., Riris, H., Mao, J., Allan, G. R., Hasselbrack, W. E., Weaver, C. J., Browell, E. W.: Airborne Measurements of CO_2 Column Concentration and Range using a Pulsed Direct-Detection IPDA Lidar, Optical Remote Sensing of the Atmosphere, 6(1), 443-469; doi:10.3390/rs6010443, 2014.

Abshire, J. B., Ramanathan, A. K., Riris, H., Allan, G. R., Sun, X., Hasselbrack, W. E., Mao, J., Wu, S., Chen, J., Numata, K., Kawa, S. R., Yang, M. Y. M., and DiGangi, J.: Airborne measurements of CO_2 column concentrations made with a pulsed IPDA lidar using a multiple-wavelength-locked laser and HgCdTe APD detector, Atmos. Meas. Tech., 11, 2001–2025, https://doi.org/10.5194/amt-11-2001-2018, 2018.

Andela, N., Morton, D. C., Giglio, L., Chen, Y., van der Werf, G. R., Kasibhatla, P. S., DeFries, R. S., Collatz, G. J., Hantson, S., Kloster, S., Bachelet, D., Forrest, M., Lasslop, G., Li, F., Mangeon, S., Melton, J. R., Yue, C., & Randerson, J. T. (2017). A human-driven decline in global burned area. Science (New York, N.Y.), 356(6345), 1356–1362. https://doi.org/10.1126/science.aal4108

Andreae, M. O.: Emission of trace gases and aerosols from biomass burning – an updated assessment, Atmos. Chem. Phys., 19,8523–8546, https://doi.org/10.5194/acp-19-8523-2019, 2019.

Bosilovich, Michael G.: Regional Climate and Variability of NASA MERRA and Recent Reanalyses: U.S. Summertime Precipitation and Temperature, J. Appl. Meteor. Climatol., 52, 1939–1951. doi: http://dx.doi.org/10.1175/JAMC-D-12-0291, 2013.

Butz, A., Hasekamp, O.P., Frankenberg, C., and Aben, I.: Retrievals of atmospheric CO_2 from simulated space-borne measurements of backscattered near-infrared sunlight: accounting for aerosol effects, Appl. Opt., 48, 3322–3336, 2009.

Ciais, P., Sabine, C., Bala, G., Bopp, L., Brovkin, V., Canadell, J., Chhabra, A., DeFries, R., Galloway, J., Heimann, M., Jones, C., Quéré, C. L., Myneni, R. B., Piao, S., and Thornton, P.: Carbon and Other Biogeochemical Cycles, chap. 6 , in: IPCC, Climate Change 2013: The Physical Science Basis. Contribution of Working Group I to the Fifth Assessment Report of the Intergovernmental Panel on Climate Change, edited by: Stocker, T. F., Qin, D., Plattner, G.-K., Tignor, M., Allen, S. K., Boschung, J., Nauels, A., Xia, Y., Bex, V., and Midgley, P. M., 465–570, Cambridge University Press, Cambridge, UK and New York, NY, USA, 2013.

Clough, S. A., Iacono, M. J. & Moncet, J.: Line-by-line calculations of atmospheric fluxes and cooling rates: Application to water vapor. J. Geophys. Res. Atmos. 97, 15,761-715,785, 1992.

Clough, S. A. & Iacono, M. J.: Line-by-line calculation of atmospheric fluxes and cooling rates 2. Application to carbon dioxide, methane, nitrous oxide and the halocarbons. J. Geophys. Res. Atmos. 100, 16,519-516,535, 1995.

Crisp, D., Atlas, R.M., Breon, F.-M., Brown, L.R., Burrows, J.P., Ciais, P., Connor, B.J., Doney, S.C., Fung, I.Y., Jacob, D.J., Miller, C.E., O'Brien, D., Pawson, S., Randerson, J.T., Rayner, P., Salawitch, R.J., Sander, S.P., Sen, B., Stephens, G.L., Tans, P.P., Toon, G.C., Wennberg, P.O., Wofsy, S.C., Yung, Y.L., Kuang, Z., Chudasama, B., Sprague, G., Weiss, B., Pollock, R., Kenyon, D., and Schroll, S.,: The Orbiting Carbon Observatory (OCO) Mission. Advances in Space Research, 34(4), 700-709, 2004.

Darmenov, A. and da Silva, A., *The Quick Fire Emissions Dataset (QFED): Documentation of versions 2.1, 2.2 and 2.4*, NASA Technical Report Series on Global Modeling and Data Assimilation NASA TM-2015-104606, Volume 38, http://gmao.gsfc.nasa.gov/pubs/docs/Darmenov796.pdf, 2015.

Diskin, G. S., Podolske, J. R., Sachse, G. W., and Slate, T. A., Open-path airborne tunable diode laser hygrometer, Proc. SPIE 4817, Diode Lasers and Applications in Atmospheric Sensing, (23 September 2002); https://doi.org/10.1117/12.453736

Duran, 2017, https://globalnews.ca/news/3921710/b-c-year-in-review-2017-wildfires/

Guerlet, S., Butz, A., Schepers, D., Basu, S., Hasekamp, O. P., Kuze, A., Yokota, T., Blavier, J.-F., Deutscher, N. M., Griffith, D. W. T., Hase, F., Kyro, E., Morino, I., Sherlock, V., Sussmann, R., Galli, A., and Aben, I.: Impact of aerosol and thin cirrus on retrieving and validating XCO_2 from GOSAT shortwave infrared measurements, J. Geophys. Res., 118, 4887-4905, doi:10.1002/jgrd.50332, 2013.

Halliday, H. S., DiGangi, J. P., Choi, Y., Diskin, G. S., Pusede, S. E., Rana, M., Nowak, J. B., Knote, C., Ren, X., He, H., Dickerson, R. R. and Li, Z.: Using short-term CO/CO 2 ratios to assess air mass differences over the Korean Peninsula during KORUS-AQ, J. Geophys. Res. Atmospheres, 124(20), 10951–10972, doi:10.1029/2018JD029697, 2019.

Houweling, S., Hartmann, W., Aben, I., Schrijver, H., Skidmore, J., Roelofs, G.-J., and Breon, F.-M.: Evidence of systematic errors in SCIAMACHY-observed CO_2 due to aerosols, Atmos. Chem. Phys., 5, 3003–3013, doi:10.5194/acp-5-3003-2005, 2005.

Kawa, S. R., Erickson, D. J. III, Pawson, S. and Zhu, Z.: Global CO_2 transport simulations using meteorological data from the NASA data assimilation system. J. Geophys. Res. 109, D18312, doi:10.1029/2004JD004554, 2004.

Kawa, S. R., J. Mao, J. B. Abshire, G. J. Collatz, X. Sun, and Weaver, C. J.: Simulation studies for a space-based CO_2 lidar mission, Tellus B, 62: 770–783. doi: 10.1111/j.1600-0889.2010.00486.x, 2010.

Kawa, S. R., Abshire, J. B., Baker, D. F., Browell, E. V., Crisp, D., Crowell, S. M. R., Hyon, J. J., Jacob, J. C., Jucks, K. W., Lin, B., et al.: Active Sensing of CO_2 Emissions over Nights, Days, and Seasons (ASCENDS): Final Report of the ASCENDS Ad Hoc Science Definition Team, Document ID: 20190000855, NASA/TP–2018-219034, GSFC-E-DAA-TN64573, 2018.

Kuze, A., Suto, H., Shiomi, K., Kawakami, S., Tanaka, M., Ueda, Y., et al., Update on GOSAT TANSO-FTS performance, operations, and data products after more than 6 years in space, Atmos. Meas. Tech., 9, 2445–2461, 2016.

Lombrana, L. M., Warren, H., Rathi, A., Measuring the Carbon-Dioxide Cost of Last Year's Worldwide Wildfires, https://www.bloomberg.com/graphics/2020-fire-emissions/

Le Quéré, C., Andrew, R. M., Friedlingstein, P., Sitch, S., Hauck, J., Pongratz, J., Pickers, P. A., Korsbakken, J. I., Peters, G. P., Canadell, J. G., Arneth, A., Arora, V. K., Barbero, L., Bastos, A., Bopp, L., Chevallier, F., Chini, L. P., Ciais, P., Doney, S. C., Gkritzalis, T., Goll, D. S., Harris, I., Haverd, V., Hoffman, F. M., Hoppema, M., Houghton, R. A., Hurtt, G., Ilyina, T., Jain, A. K., Johannessen, T., Jones, C. D., Kato, E., Keeling, R. F., Goldewijk, K. K., Landschützer, P., Lefèvre, N., Lienert, S., Liu, Z., Lombardozzi, D., Metzl, N., Munro, D. R., Nabel, J. E. M. S., Nakaoka, S.-I., Neill, C., Olsen, A., Ono, T., Patra, P., Peregon, A., Peters, W., Peylin, P., Pfeil, B., Pierrot, D., Poulter, B., Rehder, G., Resplandy, L., Robertson, E., Rocher, M., Rödenbeck, C., Schuster, U., Schwinger, J., Séférian, R., Skjelvan, I., Steinhoff, T., Sutton, A., Tans, P. P., Tian, H., Tilbrook, B., Tubiello, F. N., van der Laan-Luijkx, I. T., van der Werf, G. R., Viovy, N., Walker, A. P.,Wiltshire, A. J., Wright, R., Zaehle, S., and Zheng, B.: Global Carbon Budget 2018, Earth Syst. Sci. Data, 10, 2141–2194, https://doi.org/10.5194/essd-10-2141-2018, 2018.

Mao, J. and Kawa, S. R.: Sensitivity studies for space-based measurement of atmospheric total column carbon dioxide by reflected sunlight. Applied Optics 43, 914-927, 2004.

Mao, J., Ramanathan, A., Abshire, J. B., Kawa, S. R., Riris, H., Allan, G. R., Hasselbrack, W. E., Sun, X., Chen, J., and Numata, K.: Atmospheric CO_2 concentration measurements to cloud tops from airborne lidar measurement during ASCENDS science campaigns, Atmos. Meas. Tech., 11, 127-140, 2018.

Mao, J., Abshire, J. B., Kawa, S. R., Riris, H., Allan, G. R., Hasselbrack, W. E., Sun, X., Chen, J., Numata, K., Sun, X., Nicely, J. M., GiGang, J. P. and Choi, Y.: CO_2 Laser Sounder Lidar: Toward Atmospheric CO2 Measurements with High-precision, Low-bias and Global coverage. A43D-01 presented at the Fall Meeting, AGU, San Francisco, CA, 9-13 Dec. 2019.

Meyer, C. P., Cook, G. D., Reisen, F., Smith, T. E. L., Tattaris, M.,Russell-Smith, J., Maier, S. W., Yates, C. P., and Wooster, M. J.: Direct measurements of the seasonality of emission factors from savanna fires in northern Australia, J. Geophys. Res. Atmos.,117, D20305, https://doi.org/10.1029/2012JD017671, 2012.

Obland, M. D., A. M. Corbett, B. Lin, B. Meadows, J. F. Campbell, S. Kooi, T. Fan, W. Carrion, J. Hicks, J. Sparrow, E. V. Browell, J. Dobler, and J. DiGangi, "Advancements towards active remote sensing of CO_2 from space using intensity-modulated, continuous-Wave (IM-CW) lidar," Proc. SPIE 10785, Sensors, Systems, and Next-Generation Satellites XXII, 1078509 (2018); https://doi.org/10.1117/12.2325816

Parazoo, N., A. S. Denning, S. R. Kawa, K. Corbin, R. Lokupitia, I. Baker, and D. Worthy, Mechanisms for synoptic transport of CO_2 in the midlatitudes and tropics, Atmos. Chem. Phys., 8, 7239–7254, doi:10.5194/acp-8-7239-2008, 2008.

Ramanathan, A. K., Mao, J., Abshire, J., and Allan, G. R.: Remote sensing measurements of the CO_2 mixing ratio in the planetary boundary layer using cloud slicing with airborne lidar, Geophys. Res. Lett., 42, 2055-2062, 2015.

Ramanathan, A. K., Nguyen, H. M., Sun, X., Mao, J., Abshire, J. B., Hobbs, J. M., and Braverman, A. J.: A singular value decomposition framework for bias-free retrievals with vertical distribution information from column greenhouse gas absorption spectroscopy measurements, Atmos. Meas. Tech., 11, 4909-4928, 2018.

Rienecker, M.M., Suarez, M.J., Gelaro, R.; Todling, R., Bacmeister, J., Liu, E.; Bosilovich, M.G., Shubert, S.D., Takacs, L., Kim, G.-K., et al.: MERRA: NASA’s modern-era retrospective analysis for research and applications. J. Clim., 24, 3624–3648, 2011.

Rothman, L., et al.: The HITRAN 2008 molecular spectroscopic database, J. Quant. Spectros. Radiat. Transfer, 110(9), 533–572, 2009.

Sun, X., Abshire, J. B., Ramanathan, A., Kawa, S. R., and Mao, J.: Retrieval Algorithm for the Column CO_2 Mixing Ratio from Pulsed Multi-Wavelength Lidar Measurements. Atmos. Meas. Tech. 14, 3909–3922, https://doi.org/10.5194/amt-14-3909-2021, 2021.

Tian, H., Lu, C., Ciais, P., Michalak, A. M., Canadell, J. G., Saikawa, E., Huntzinger, D. N., Gurney, K. R., Sitch, S., Zhang, B., Yang, J., Bousquet, P., Bruhwiler, L., Chen, G., Dlugokencky, E., Friedlingstein, P., Melillo, J., Pan, S., Poulter, B., Prinn, R., Saunois, M., Schwalm, C. R., and Wofsy, S. C.: The terrestrial biosphere as a net source of greenhouse gases to the atmosphere, Nature, 531, 225–228, https://doi.org/10.1038/nature16946, 2016.

Torres, O., Bhartia, P. K., Taha, G., Jethva, H., Das, S., Colarco, P., et al. (2020). Stratospheric injection of massive smoke plume from Canadian boreal fires in 2017 as seen by DSCOVR‐EPIC, CALIOP, and OMPS‐LP observations. Journal of Geophysical Research: Atmospheres, 125, e2020JD032579. https://doi.org/10.1029/2020JD032579

Uchino, O., Kikuchi, N., Sakai, T., Morino, I., Yoshida, Y., Nagai, T., Shimizu, A., Shibata, T., Yamazaki, A., Uchiyama, A., Kikuchi, N., Oshchepkov, S., Bril, A., and Yokota, T.: Influence of aerosols and thin cirrus clouds on the GOSAT-observed CO_2: a case study over Tsukuba, Atmos. Chem. Phys., 12, 3393-3404, doi:10.5194/acp-12-3393-2012, 2012.

van der Werf, G. R., Randerson, J. T., Giglio, L., van Leeuwen, T. T., Chen, Y., Rogers, B. M., Mu, M., van Marle, M. J. E., Morton, D. C., Collatz, G. J., Yokelson, R. J., and Kasibhatla, P. S.: Global fire emissions estimates during 1997–2016, Earth Syst. Sci. Data, 9, 697–720, https://doi.org/10.5194/essd-9-697-2017, 2017.

Wunch, D., Toon, G. C., Blavier, J.-F. L., Washenfelder, R. A., Notholt, J., Connor, B. J., Griffith, D. W. T., Sherlock, V., and Wennberg, P. O.: The total carbon column observing network, Philos. T. R. Soc. A, 369, 2087–2112, doi:10.1098/rsta.2010.0240, 2011.